



Photophysical and photochemical insights into the photodegradation of sulfapyridine in water: A joint experimental and theoretical study



Heming Zhang^a, Xiaoxuan Wei^b, Xuedan Song^a, Shaheen Shah^a, Jingwen Chen^c, Jianhui Liu^a, Ce Hao^{a,*}, Zhongfang Chen^{b,*}

^a State Key Laboratory of Fine Chemicals, Dalian University of Technology, Dalian 116024, China

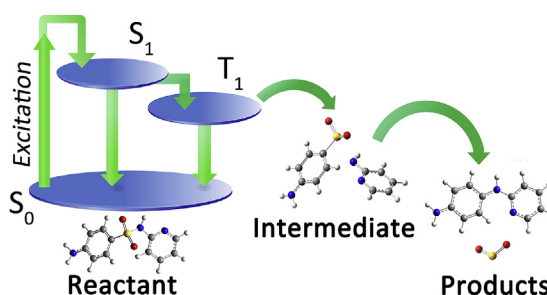
^b Department of Chemistry, University of Puerto Rico, Rio Piedras Campus, San Juan, PR 00931, USA

^c Key Laboratory of Industrial Ecology and Environmental Engineering (MOE), School of Environmental Science and Technology, Dalian University of Technology, Dalian 116024, China

HIGHLIGHTS

- Systematically simulate both photophysical and photochemical processes of sulfapyridine.
- The rate constants for each photophysical process were calculated, the photoreaction mechanism was revealed.
- The theoretically predicted photodegradation rate constant agrees well with our experimental measurement.
- Theoretically predict the reaction quantum yield and the photodegradation rate constant under certain light irradiation.

GRAPHICAL ABSTRACT



ARTICLE INFO

Article history:

Received 3 August 2017

Received in revised form

5 October 2017

Accepted 6 October 2017

Available online 7 October 2017

Handling Editor: Jun Huang

Keywords:

Photodegradation

Sulfapyridine

Water treatment

Photophysical and photochemical processes

ABSTRACT

For organic pollutants, photodegradation, as a major abiotic elimination process and of great importance to the environmental fate and risk, involves rather complicated physical and chemical processes of excited molecules. Herein, we systematically studied the photophysical and photochemical processes of a widely used antibiotic, namely sulfapyridine. By means of density functional theory (DFT) computations, we examined the rate constants and the competition of both photophysical and photochemical processes, elucidated the photochemical reaction mechanism, calculated reaction quantum yield (Φ) based on both photophysical and photochemical processes, and subsequently estimated the photodegradation rate constant. We further conducted photolysis experiments to measure the photodegradation rate constant of sulfapyridine. Our computations showed that sulfapyridine at the lowest excited singlet state (S_1) mainly undergoes internal conversion to its ground state, and is difficult to transfer to the lowest excited triplet states (T_1) via intersystem crossing (ISC) and emit fluorescence. In T_1 state, compared with phosphorescence emission and ISC, chemical reaction is much easier to initiate. Encouragingly, the theoretically predicted photodegradation rate constant is close to the experimentally observed value, indicating that quantum chemistry computation is powerful enough to study photodegradation involving ultra-fast photophysical and photochemical processes.

© 2017 Elsevier Ltd. All rights reserved.

* Corresponding author.

** Corresponding author.

E-mail addresses: haoce@dlut.edu.cn (C. Hao), zhongfangchen@gmail.com (Z. Chen).

1. Introduction

Photodegradation, which can irreversibly alter the structure of organic molecules by light, is a major abiotic elimination process for organic pollutants. Various experimental studies showed that many organic pollutants, e.g., pharmaceuticals and personal care products, can undergo photodegradation under sunlight or simulated sunlight irradiation (Bonvin et al., 2013; Boreen et al., 2003; Kelly and Arnold, 2012; Wang and Lin, 2012; Yan and Song, 2014). For example, fluoroquinolone antibiotics can photodegrade via defluorination, cleavage of the piperazine ring and decarboxylation in natural water with short half-lives of a few minutes (Wei et al., 2013).

Organic pollutants with different structures may have distinct photolytic mechanisms and kinetics constants. For example, sulfonamides with five-membered heterocyclic groups mainly undergo photocleavage, while sulfonamides with six-membered heterocyclic groups mainly photodegrade to SO₂ extrusion products, concomitantly the photolytic quantum yields (Φ) of the former are about 2–3 orders of magnitude higher than those of the latter (Boreen et al., 2004, 2005).

Given the huge and ever-increasing number of organic pollutants (Schwarzenbach et al., 2006), it is necessary to evaluate their photodegradation, that involves numerous photophysical and photochemical processes, by computational approaches, as the speed of experimental determination of photodegradation lags behind the speed of pollutants that emerge, and experimental determination usually requires high expenditure and expensive equipments. Recently, quantum chemistry methods have been employed to clarify the mechanisms of photochemical processes. For example, by means of density functional theory (DFT) computations, Wei et al. (2013) discovered that the photoinduced defluorination of ciprofloxacin at the lowest excited triplet state (T_1) is mainly induced by OH[−] addition. Sun et al. (2015) investigated the ·OH radical-initiated oxidation degradation of N-ethylperfluorobutyramide, and Li et al. (2016b) examined the catalytic mechanism of C–F bond cleavage of fluoroacetate dehalogenase. However, photophysical processes have been generally ignored in previous studies. As shown in Fig. 1, photophysical processes are clarified by a Jablonski diagram. An organic compound can be excited from its ground state (S_0) to excited singlet states (S_n , $n \geq 1$) after the sunlight absorption and fall to S_1 state. Organics in S_1 states can go back to the S_0 state by internal conversion (IC) and fluorescence emission (F), and transfer to excited triplet states (T_1)

via intersystem crossing (ISC). In T_1 states, organics can deactivate through phosphorescence emission (P) and ISC back to S_0 state, and also can undergo primary chemical reactions. Illustrating the transition rate constants and competition of these processes can reveal many valuable information, for example the quantum yield, which measures how efficiently a compound reacts upon absorption of a photon, is an important parameter when studying organic photo-degradation (Boreen et al., 2004, 2005; Wei et al., 2013). Thus, to grasp the overall picture of the photodegradation of a certain organic, it is necessary to study both photophysical and photochemical processes.

In this study, we selected a widely used and highly detected sulfonamide antibiotic namely sulfapyridine (detected in effluent at 63–135 ng/l by Göbel et al., 2004) as a case to systematically simulate its photophysical and photochemical processes. The rate constants for each photophysical process of sulfapyridine were calculated, their competition were discussed, and the photoreaction mechanism was revealed. Based on the understanding of each photophysical and photochemical process and their overall competition, we evaluated the photolytic reaction quantum yields (Φ), and further estimated the photodegradation rate constant of sulfapyridine based on the reaction quantum yields and other experimental data. The validity of our prediction procedure was confirmed by the good agreement between the theoretically predicted and the experimentally measured photodegradation rate constants.

2. Methods and materials

2.1. Computational details

All the geometry optimizations and frequency analyses were carried out with the Gaussian 09 program package (Frisch et al., 2009), using the B3LYP functional (Silva-Junior et al., 2008; Jacquemin et al., 2010) in conjunction with the 6-31 + G(d,p) basis set. Solvent effect of water was considered by the integral equation formalism of polarized continuum model (IEFPCM) based on the self-consistent-reaction-field (SCRF) method (Tomasi et al., 2005). The geometries of sulfapyridine at the S_0 and T_1 states were calculated at spin multiplicities of 1 and 3, respectively (Nozaki et al., 2006). While for the sulfapyridine at the lowest excited singlet state (S_1), the geometry optimization and frequency calculation were performed using time-dependent density functional theory (TD-DFT). No significant differences were found between the computed and experimentally measured key geometric parameters of sulfapyridine (see Table S1 in Supporting Information, SI), indicating the reliability of the selected methods for the system under study.

For the photophysical processes, we computed the transition electronic dipole moment of fluorescence emission and the electronic transition field required for IC at the same level of theory as that for geometry optimization with Gaussian 09 program. Transition electronic dipole moment of phosphorescence emission and spin-orbit coupling constant of ISC were computed by ADF2013 program package (ADF 2013, SCM, Theoretical Chemistry, Vrije Universiteit, Amsterdam, The Netherlands, <http://www.scm.com>; Fonseca et al., 1998; Te Velde et al., 2001) with the method of scalar zero-order regular approximation (ZORA) (Van Lenthe et al., 1993, 1994, 1996a, 1996b, 1999) at TD-DFT/B3LYP/Aug-DZP level of theory. The agreement between the calculated and experimentally measured fluorescence spectrum of sulfapyridine (shown in Fig. S2) validates the rigidity of our theoretical methods to describe the behaviors at excited states. Rate constants of photophysical transitions were computed via MOMAP program (Niu et al., 2008, 2010; Peng et al., 2007, 2013).

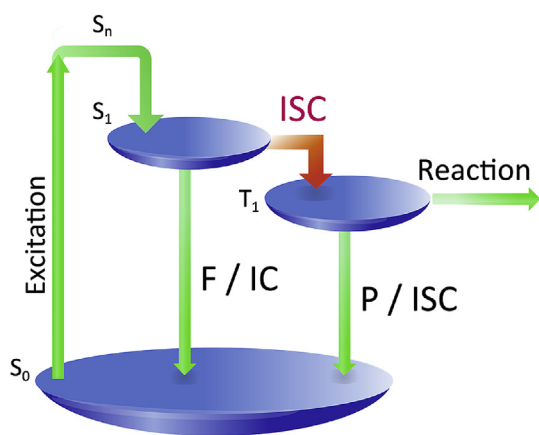


Fig. 1. Simplified Jablonski diagram. S_0 : ground state; S_n ($n \geq 1$): excited singlet states; T_n ($n \geq 1$): excited triplet states; F: fluorescence emission; IC: internal conversion; P: phosphorescence emission; ISC: intersystem crossing.

According to previous studies (Albini and Monti, 2003; Ji et al., 2013; Li et al., 2016a) and our photolytic experiments (Fig. S3), we theoretically studied the photochemical reactions of sulfapyridine in triplet state. Based on the photoproducts detected for sulfonamides (Challis et al., 2013; García-Galán et al., 2012), reaction paths were searched. The nature of stationary points was determined by frequency calculations, and the transition states (TS) were characterized by only one imaginary vibrational frequency. The intrinsic reaction coordinate (IRC) analysis (Fukui, 1981) was executed to verify that each TS uniquely connects the reactants with products. The potential energy surface profiles include zero-point energy and thermal energy corrections. The spin densities were evaluated by the Hirshfeld analysis (Hirshfeld, 1977).

2.2. Chemicals and experimental methods

Sulfapyridine (98.0% purity) and Sorbic acid (99%) were purchased from Tokyo Chemical Industry CO., Ltd. and J&K Scientific Ltd., respectively. Ultrapure water (18 MΩ cm) was obtained from an OKP ultrapure water system produced by Shanghai Lakecore Instrument Co., Ltd.

Photolytic experiments were performed with an XPA-7 merry-go-round photochemical reactor from Xujiang Electromechanical Plant, Nanjing, China. A water-refrigerated 500 W mercury lamp surrounded by 290 nm cut-off filters was used as the light source ($\lambda > 290$ nm). The equilibrium temperature of the photolytic system was around 35 °C adjusted by an air cooling system. The spectra of the light source were measured by a spectroradiometer with a RAMSES-ACC-UV sensor from TriOS CO., Ltd., Germany. During the photolytic processes, aqueous solution of sulfapyridine (5 μmol/L, pH = 6.5) was placed into quartz tubes.

The concentration of sulfapyridine was determined by a Hitachi L-2000 HPLC with an Agilent Eclipse XDB-C18 column (4.6 × 150 mm, 5 μm) and a L-2455 diode array detector (detection wavelength: 260 nm). The mobile phase consisted of 20% acetonitrile and 80% ammonium acetate buffered water (pH = 5). The flow rate was 0.8 mL/min, injection volume was 20 μL, and column temperature was 25 °C. Fluorescence spectrum of sulfapyridine was detected by Spectrofluorometer FS5 fluorescence spectrometer produced by Edinburgh Instruments, EI. The light slit in the measurement of fluorescence emission spectrum was set to 5 nm and the excitation wavelength was 310 nm. To obtain enough signals, the concentration of sulfapyridine in the fluorescence emission spectrum measurement was increased to 40 mg/L (0.16 mmol/L).

3. Results and discussion

3.1. Competitive processes of sulfapyridine in S_1 state

According to the Kasha's rule (1950), the photophysical and photochemical processes of sulfapyridine can be dictated by the lowest-lying excited state (S_1 and T_1 states). For sulfapyridine in S_1 state, there are three competitive processes, namely fluorescence emission, internal conversion (IC), and intersystem crossing (ISC). Based on Fermi's golden rule, the rate constants of these three processes can be described by as follows (Lin, 1966):

$$k_{if} = \frac{2\pi}{\hbar} |\langle \psi_i | V | \psi_f \rangle|^2 \rho(E_f) \quad (1)$$

where i and f represent the initial and final states, respectively; \hbar is the reduced Planck constant, $\hbar = h/2\pi$, h is the Planck constant; ψ is the wave function which can describe the state of system; V is the electronic coupling, which depends on the nature of the process; ρ and E stand for the density and energy of states, respectively.

Considering time-dependent perturbation and Franck-Condon approximation, emission spectrum can be considered as a differential of the dipole-allowed spontaneous photon emission rate, $\sigma_{em}(\omega)$ (Niu et al., 2010; Peng et al., 2007):

$$\sigma_{emi}(\omega, T) = \frac{4\omega^3}{3\hbar c^3} \sum_{v_i, v_f} P_{i, v_i}(T) \left| \langle \Theta_{f, v_f} | \vec{\mu}_0 | \Theta_{i, v_i} \rangle \right|^2 \delta(\omega_{iv_i, fv_f} - \omega) \quad (2)$$

where ω is the circular frequency; c is speed of light in vacuum; $P_{i, v_i}(T)$ is the Boltzmann distribution function for the initial vibronic manifold; v_i and v_f are the quantum number of the initial and final vibrational modes, respectively; T is temperature, $\vec{\mu}_0$ is the electric transition dipole moment; Θ is the vibrational wave function, and δ is the Dirac operator. Thus, the rate constant of fluorescence emission (k_F) can be calculated by the integration of $\sigma_{em}(\omega)$ (Niu et al., 2010):

$$k_F \text{ (or } k_p) = \int_0^{+\infty} \sigma_{em}(\omega) d\omega \quad (3)$$

And the rate constants of IC (k_{IC}) (Niu et al., 2008) and ISC (k_{ISC}) (Peng et al., 2013) can be calculated as follows:

$$k_{IC} = \frac{2\pi}{\hbar} \sum_{v_i, v_f} P_{i, v_i}(T) \left| \sum_n \langle \Phi_f | \hat{P}_n | \Phi_i \rangle \langle \Theta_{f, v_f} | \hat{P}_n | \Theta_{i, v_i} \rangle \right|^2 \delta(E_{i, v_i} - E_{f, v_f}) \quad (4)$$

$$k_{ISC} = \frac{2\pi}{\hbar} \sum_{v_i, v_f} P_{i, v_i}(T) \left| \langle \Phi_f \Theta_{f, v_f} | \hat{H}_{SO} | \Phi_i \Theta_{i, v_i} \rangle \right|^2 \delta(E_{i, v_i} - E_{f, v_f}) \quad (5)$$

where n is the index of normal mode; Φ is the electron wave function; \hat{P}_n is the momentum operator of the n th normal mode in the final electronic state; \hat{H}_{SO} is the spin-orbit coupling Hamilton operator.

We first computed the rate constants of fluorescence emission (k_F), internal conversion (k_{IC}), intersystem crossing (k_{ISC, S_1-T_1}) for sulfapyridine at the S_1 state (see Table 1). Among these rate constants, the k_{IC} value is the largest, and is “two” orders of magnitude higher than k_F and “four” orders of magnitude higher than k_{ISC, S_1-T_1} , indicating that sulfapyridine in S_1 state mainly undergoes IC and deactivates to S_0 state. The relatively small k_F value ($2.2 \times 10^6 \text{ s}^{-1}$) suggests that the fluorescence emission of sulfapyridine is weak. This predicted weak fluorescence emission well explains why pre-column derivatization with fluorescamine is commonly used to markedly increase the fluorescence detection sensitivity of sulfapyridine in very low concentration (Maudens et al., 2004; Stoev and Michailova, 2000; Schwaiger and Schuch, 2000), which also suggests the reliability of our computational method. The rate constant k for ISC is smallest ($8.4 \times 10^3 \text{ s}^{-1}$ for the $S_1 \rightarrow T_1$ process), indicating that the transition from the S_1 state to T_1 state is difficult. Since the photochemical reaction of sulfapyridine mainly occurs at triplet state, ISC($S_1 \rightarrow T_1$) is suspicious to be the bottleneck for the photodegradation of sulfapyridine. However, the final answer can only be reached after we also clarify the rate-limiting step of the photochemical reaction.

By comparing the vertical electronic excitation energies of the optimized S_1 geometry (listed in Table S2), we found that the T_2 state is 0.23 eV higher in energy than that of the S_1 state, while energetically the S_1 and T_1 states are close and T_1 is just 0.01 eV below S_1 state. Thus, ISC from S_1 to T_1 is the main intersystem crossing, and we only considered ISC from S_1 to T_1 for further

Table 1

Rate constants of fluorescence emission (k_F), internal conversion (k_{IC}), intersystem crossing (k_{ISC}), phosphorescence emission (k_P) and photochemical reactions for sulfapyridine.

Competitive processes in S_1 state		Competitive processes in T_1 state	
k_F	$2.2 \times 10^6 \text{ s}^{-1}$	k_P	$5.8 \times 10^{-4} \text{ s}^{-1}$
k_{IC}	$1.5 \times 10^8 \text{ s}^{-1}$	$k_{ISC,T1-S0}$	$3.7 \times 10^7 \text{ s}^{-1}$
$k_{ISC,S1-T1}$	$8.4 \times 10^3 \text{ s}^{-1}$	k_R	$2.1 \times 10^{12} \text{ s}^{-1}$; $9.3 \times 10^{-6} \text{ s}^{-1}$

studies in this work.

3.2. Competitive processes of sulfapyridine in T_1 state

At T_1 state, besides phosphorescence emission and intersystem crossing as two photophysical processes, sulfapyridine also can undergo photochemical reactions. Thus, we computed the rate constants of phosphorescence emission (k_P), intersystem crossing ($k_{ISC,T1-S0}$), and photochemical reactions (k_R) for sulfapyridine in T_1 state (see Table 1).

To calculate the rate constant of photochemical reactions (k_R), the reaction mechanism was studied. We examined two possible SO_2 -extrusion reaction pathways, passing transition states of TS_{2A} and TS_{2B} respectively (Fig. 2) based on the photoproducts detected experimentally for sulfonamides (Challis et al., 2013; García-Galán et al., 2012). Both reaction pathways are initiated by the elongation of the S–N₁ bond: in the reactant (R), the S–N₁ bond is 1.78 Å, after crossing a small activation barrier (0.6 kcal/mol), the S–N₁ bond is ruptured with a distance of 4.25 Å in the intermediate (IM). Subsequently, there are two possible pathways: in Path A, the carbon atom C₁ (connected with SO_2 group) attack N₁ by crossing a 20.3 kcal/mol barrier, and the C₁–N₁ bond is reduced to 1.36 Å in the product P_A; in Path B, the C₁ atom attacks N₂ by crossing a 37.9 kcal/mol barrier, forming a C₁–N₂ bond of 1.42 Å in the product P_B. In both pathways, the S–C₁ bond cleavage occurs, resulting in the SO_2 extrusion product and SO_2 (see Fig. 2).

As indicated by the calculated activation energies (E_a) in Fig. 2(a), for the first step, $E_{a,1}$ (0.6 kcal mol^{−1}) is much smaller than the $E_{a,2}$ in the second step. For the second step, Path A has a much lower activation barrier (20.3 kcal/mol) than that in Path B (37.9 kcal/mol). Thus, sulfapyridine in T_1 state mainly undergoes Path A to form P_A and SO_2 . The preference of Path A over Path B can also be revealed from the spin density distribution on N₁ (ρ_{N1}), and N₂ (ρ_{N2}), atoms. ρ_{N1} increases from 0.05 in R to 0.52 in IM, indicating that a N₁-centered radical is formed in IM; in comparison, ρ_{N2} is only 0.13 on N₂ atom in IM. Generally, the higher spin density may result in more facile reaction, thus it is easy to understand why the N₁ site with stronger radical character exhibits higher activity than N₂. In addition, the product (the complex of P_A and SO_2) of Path A is 28.8 kcal/mol lower in energy than that of Path-B, indicating that Path A is also thermodynamically more favorable. Therefore, P_A is preferred both kinetically and thermodynamically, and is the main product of photodegradation. Note that García-Galán et al. (2012) also identified P_A as a main photoproduct for sulfapyridine experimentally, while P_B was not detected, which confirms that the major reaction pathway found in this work is reasonable.

We further computed the Gibbs free energies of activation (ΔG^\ddagger) of the elementary reaction steps for sulfapyridine in T_1 state following both reaction pathways. The ΔG^\ddagger value (0.7 kcal/mol) for the first step is very small. For the second step, ΔG^\ddagger values in Path A and Path B are 25.2 and 43.5 kcal/mol, respectively. Based on these ΔG^\ddagger values, we can estimate the rate constants of the two

elementary reaction steps in the major reaction Path A (k_{R1} and $k_{R,2A}$) as (Eyring, 1935):

$$k_R = \kappa_i \frac{k_B T}{h} \exp\left(-\frac{\Delta G^\ddagger}{RT}\right) \quad (6)$$

where k_B and h are Boltzmann and Planck constants, respectively; κ_i is transmission coefficient. κ_i can be calculated as (Louis et al., 2000):

$$\kappa_i = 1 + \frac{1}{24} \left(\frac{h\nu_i}{k_B T}\right)^2 \quad (7)$$

where ν_i is the imaginary frequency of TS. The value of k_{R1} and k_{R2} were calculated to be $2.1 \times 10^{12} \text{ s}^{-1}$ and $9.3 \times 10^{-6} \text{ s}^{-1}$, respectively.

By using Eqs.(3) and (5), the rate constants of phosphorescence emission (k_P) and intersystem crossing ($k_{ISC,T1-S0}$) were calculated to be $5.8 \times 10^{-4} \text{ s}^{-1}$ and $3.7 \times 10^7 \text{ s}^{-1}$, respectively. Note that the k_P value is extremely small, while rate constant for intersystem crossing in T_1 state here ($3.7 \times 10^7 \text{ s}^{-1}$) is nearly four orders of magnitude than that at the S_1 state ($8.4 \times 10^3 \text{ s}^{-1}$).

Summarizing all the calculated rate constants for the photophysical and photochemical processes of sulfapyridine in T_1 state (shown in Table 1), the competition of these processes is clear. k_P ($5.8 \times 10^{-4} \text{ s}^{-1}$) is so small and much lower than $k_{ISC,T1-S0}$ ($3.7 \times 10^7 \text{ s}^{-1}$) and k_{R1} ($2.1 \times 10^{12} \text{ s}^{-1}$), respectively. These data suggest the phosphorescence emission may not be easy, which echoes our experimental finding that no phosphorescence signal for sulfapyridine was observed in the room temperature. k_{R1} ($2.1 \times 10^{12} \text{ s}^{-1}$) is much larger than $k_{ISC,T1-S0}$ ($3.7 \times 10^7 \text{ s}^{-1}$), indicating that in T_1 state it is much easier for sulfapyridine to undergo photochemical reaction to generate IM. Subsequently, IM undergoes the second step of Path A to form the photoproducts of P_A and SO_2 with a very small $k_{R,2A}$ ($9.3 \times 10^{-6} \text{ s}^{-1}$). As discussed, the second step of Path A is the rate-limiting step of photochemical reaction. Comparing its rate constant $k_{R,2A}$ ($9.3 \times 10^{-6} \text{ s}^{-1}$) and that of ISC_{S1-T1} ($k_{ISC,S1-T1}$, $8.4 \times 10^3 \text{ s}^{-1}$), clearly the rate-limiting step in Path A is much slower than ISC ($S_1 \rightarrow T_1$), the bottleneck of photophysical process. Thus, the second step in Path A is the rate-limiting step in the overall competition between both photophysical and photochemical processes. Therefore, lowering the E_a of the photochemical reaction could be an effective strategy to enhance the direct photolysis of sulfapyridine. Other strategies, like introducing ·OH radical, to undergo reaction paths with lower E_a could also be promising (Sun et al., 2015; Li et al., 2016b).

3.3. Evaluation of reaction quantum yield and direct photolysis rate constant

The reaction quantum yield Φ is a major characteristics for an organic photodegradation process. Once Φ is obtained, it is possible to evaluate the photodegradation rate constant under certain light sources. Therefore, determining Φ is essential for us to predict the behavior of organic photodegradation (Zepp and Cline, 1977). In this work, based upon the understanding of all the competitive photophysical and photochemical processes, Φ was calculated:

$$\Phi = \frac{k_{ISC,S1-T1}}{k_F + k_{IC} + k_{ISC,S1-T1}} \times \frac{k_{R1}}{k_{R1} + k_P + k_{ISC,T1-S0}} \quad (8)$$

The theoretically calculated value of the Φ is 5.6×10^{-5} .

With this calculated Φ value, we can estimate the photodegradation rate constant of sulfapyridine. In transparent dilute solutions, the direct photolysis rate constant (k) of an organic compound can be expressed as (Zepp and Cline, 1977):

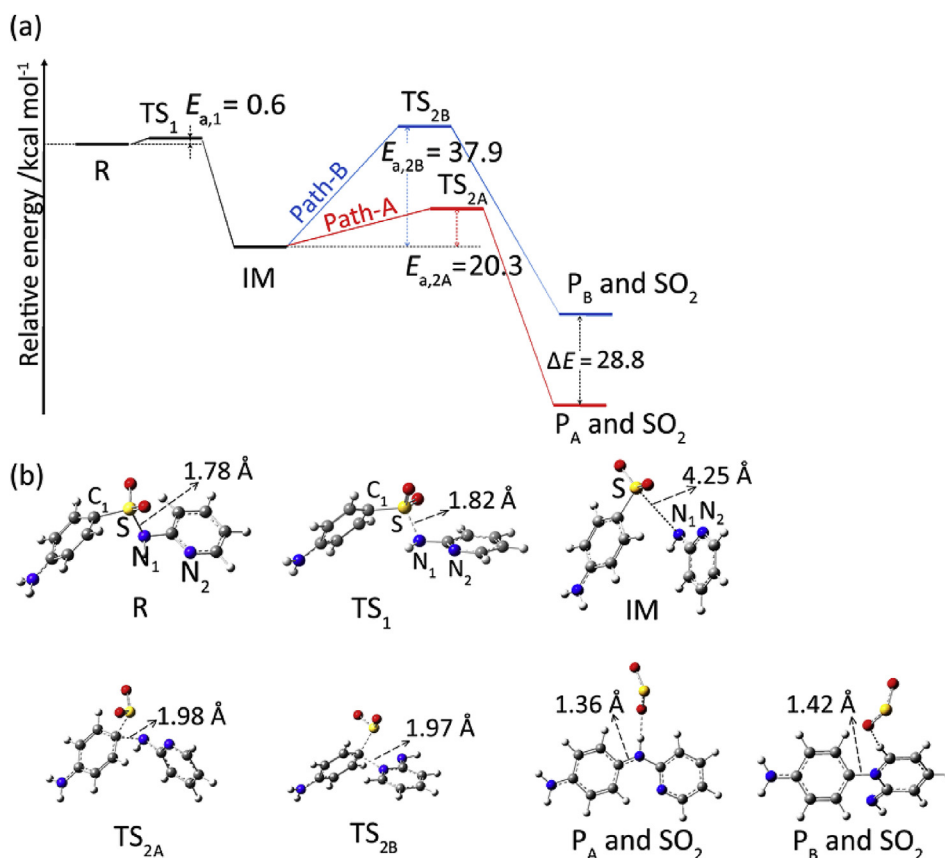


Fig. 2. Potential energy surface profiles for the photochemical reaction paths A (red line) and B (blue line) of sulfapyridine, and optimized structures of reactant (R), transition states (TS₁, TS_{2A} and TS_{2B}), intermediate (IM), and products (P_A and P_B). Dark gray atom: C; Blue atom: N; Red atom: O; Yellow atom: S; Light gray atom: H. (For interpretation of the references to colour in this figure legend, the reader is referred to the web version of this article.)

$$k = 2.303\Phi \sum L_{\lambda} \epsilon_{\lambda} \quad (9)$$

where L_{λ} is the incident light intensity at a given wavelength λ ; ϵ_{λ} is the molar absorptivity. L_{λ} and ϵ_{λ} were measured experimentally (for detailed data, refer to Table S3). When measuring the L_{λ} , the probe and the reaction tube were placed at the same position to ensure

that they receive the same light intensity. Based on Eq. (8), using the theoretical Φ value and the experimentally measured L_{λ} and ϵ_{λ} , we estimated the photodegradation rate constant k to be $3.4 \times 10^{-5} \text{ s}^{-1}$ (Refer to SI for detailed process).

To validate the theoretical estimation of the photodegradation rate constant, we conducted the photolysis experiments of sulfapyridine. Upon the light irradiation, the concentration of sulfapyridine in reaction tubes was measured at each time interval. The reaction rate of sulfapyridine was fitted into the pseudo-first order kinetic model, where the decrease of the concentration with time is proportional to the sulfapyridine concentration in the tube:

$$-\frac{dc}{dt} = kc \quad (10)$$

The correlation coefficients (r^2) of the fitting is 0.995 ± 0.003 , indicating that the direct photolysis of sulfapyridine in water obeys the pseudo-first order kinetic model (kinetics is shown in Fig. 3), and the fitted rate constant of sulfapyridine is $2.8 \times 10^{-5} \text{ s}^{-1}$. Meanwhile, no significant elimination of sulfapyridine was observed in the dark control. The difference between the calculated and experimentally measured degradation rate constants is within one order of magnitude.

Though the agreement between theoretical and experimental results is rather encouraging, we have to be aware of the approximations made in our computations. For example, Eq. (5) used to calculate the rate coefficient of ISC is a simple first-order expression, which neglects the contribution of non-adiabatic coupling. Under this treatment, only the first-order ISC coefficient is considered, but sometimes the second-order coefficient may have a

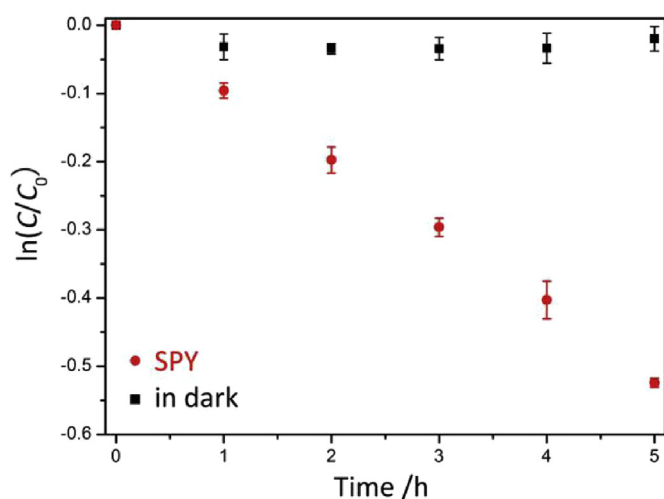


Fig. 3. Photolytic kinetics of sulfapyridine in pure water and in dark control. The error bars represent 95% confidence intervals ($n = 3$).

dominant contribution²⁸; Moreover, the triplet state reaction paths were computed by the unrestricted DFT method, while the more appropriate method to search for TS at excited state, namely TD-DFT, is still beyond our current computational capability. Therefore, more advanced computational methods are still desirable for precise predictions.

4. Conclusion

In this study, we theoretically studied both the photophysical and photochemical processes of SPY. The competition of photophysical processes reveals that ISC($S_1 \rightarrow T_1$) is the bottleneck for sulfapyridine to reach triplet state and may limit the initiation step of photochemical reaction, which is a new understanding of the low photodegradation rate of sulfapyridine in water from photophysical perspective. For the photochemical process of sulfapyridine, a mechanism of two steps and radical property of the rate-limiting step was found, which is similar with the direct photolysis mechanisms of other sulfanilamide antibiotics containing a six-membered ring in our previous works (Shah et al., 2015; Shah and Hao, 2016). The result may be instructive in the environmental assessment and elimination of this group of antibiotics.

Based on the understanding of both the photophysical and photochemical processes, quantum yield Φ was estimated for the first time and direct photodegradation rate constant was evaluated with a good agreement with experimental result. On the current stage, this work only attempted to make an estimation in a simple system taking no account of rather complicated factors in real water environment like dissolved organic matters and inorganic ions. While, faced upon with a large number of known organic pollutants in water environment and even more emerging chemicals in market, the traditional experimental determination of Φ is not efficient enough and high-throughout computational prediction can be a tendency in the future.

Acknowledgement

The financial support of the National Natural Science Foundation of China (Grant Nos. 21137001, 21677069 and 21373042) are greatly appreciated and the Fundamental Research Funds for the Central Universities of China (DUT13RC (3)013).

Appendix A. Supplementary data

Supplementary data related to this article can be found at <https://doi.org/10.1016/j.chemosphere.2017.10.036>.

References

- Albini, A., Monti, S., 2003. Photophysics and photochemistry of fluoroquinolones. *Chem. Soc. Rev.* 32 (4), 238–250.
- Bonvin, F., Omlin, J., Rutler, R., Schweizer, W.B., Alaimo, P.J., Strathmann, T.J., McNeill, K., Kohn, T., 2013. Direct photolysis of human metabolites of the antibiotic sulfamethoxazole: evidence for abiotic back–transformation. *Environ. Sci. Technol.* 47 (13), 6746–6755.
- Boreen, A.L., Arnold, W.A., McNeill, K., 2003. Photodegradation of pharmaceuticals in the aquatic environment: a review. *Aquat. Sci.* 65, 320–341.
- Boreen, A.L., Arnold, W.A., McNeill, K., 2004. Photochemical fate of sulfa drugs in the aquatic environment: sulfa drugs containing five–membered heterocyclic groups. *Environ. Sci. Technol.* 38, 3933–3940.
- Boreen, A.L., Arnold, W.A., McNeill, K., 2005. Triplet–sensitized photodegradation of sulfa drugs containing six–membered heterocyclic groups: identification of an SO_2 extrusion photoproduct. *Environ. Sci. Technol.* 39, 3630–3638.
- Challis, J.K., Carlson, J.C., Friesen, K.J., Hanson, M.L., Wong, C.S., 2013. Aquatic photochemistry of the sulfonamide antibiotic sulfapyridine. *J. Photochem. Photobiol. A* 262, 14–21.
- Eyring, H., 1935. The activated complex in chemical reactions. *J. Chem. Phys.* 3, 107.
- Fonseca, G.C., Snijders, J.G., te Velde, G., Baerends, E.J., 1998. Towards an order-N DFT method. *Theor. Chem. Acc.* 99, 391–403.
- Frisch, M.J., Trucks, G.W., Schlegel, H.B., Scuseria, G.E., Robb, M.A., Cheeseman, J.R., Scalmani, G., Barone, V., Mennucci, B., Petersson, G.A., Nakatsuji, H., Caricato, M., Li, X., Hratchian, H.P., Izmaylov, A.F., Bloino, J., Zheng, G., Sonnenberg, J.L., Hada, M., Ehara, M., Toyota, K., Fukuda, R., Hasegawa, J., Ishida, M., Nakajima, T., Honda, Y., Kitao, O., Nakai, H., Vreven, T., Montgomery, J.J.A., Peralta, J.E., Ogliaro, F., Bearpark, M., Heyd, J.J., Brothers, E., Kudin, K.N., Staroverov, V.N., Kobayashi, R., Normand, J., Raghavachari, K., Rendell, A., Burant, J.C., Iyengar, S.S., Tomasi, J., Cossi, M., Rega, N., Millam, J.M., Klene, M., Knox, J.E., Cross, J.B., Bakken, V., Adamo, C., Jaramillo, J., Gomperts, R., Stratmann, R.E., Yazyev, O., Austin, A.J., Cammi, R., Pomelli, C., Ochterski, J.W., Martin, R.L., Morokuma, K., Zakrzewski, V.G., Voth, G.A., Salvador, P., Dannenberg, J.J., Dapprich, S., Daniels, A.D., Farkas, Ö., Foresman, J.B., Ortiz, J.V., Cioslowski, J., Fox, D.J., 2009. Gaussian. Gaussian Inc., Wallingford, CT.
- Fukui, K., 1981. The path of chemical-reactions - the IRC approach. *Acc. Chem. Res.* 14 (12), 363–368.
- García-Galán, M.J., Díaz-Cruz, M.S., Barceló, D., 2012. Kinetic studies and characterization of photolytic products of sulfamethazine, sulfapyridine and their acetylated metabolites in water under simulated solar irradiation. *Water Res.* 46, 711–722.
- Göbel, A., McArdell, C.S., Suter, M.J.F., Giger, W., 2004. Trace determination of macrolide and sulfonamide antimicrobials, a human sulfonamide metabolite, and trimethoprim in wastewater using liquid chromatography coupled to electrospray tandem mass spectrometry. *Anal. Chem.* 76, 4756–4764.
- Hirshfeld, F.L., 1977. Bonded-atom fragments for describing molecular charge densities. *Theor. Chem. Acc.* 44, 129–138.
- Jacquemin, D., Perpète, E.A., Ciofini, I., Adamo, C., 2010. Assessment of functionals for TD-DFT calculations of singlet-triplet transitions. *J. Chem. Theory Comput.* 6 (5), 1532–1537.
- Ji, Y., Zhou, L., Zhang, Y., Ferronato, C., Brigante, M., Mailhot, G., Yang, X., Chovelon, J., 2013. Photochemical degradation of sunscreen agent 2-phenylbenzimidazole-5-sulfonic acid in different water matrices. *Water Res.* 47 (15), 5865–5875.
- Kasha, M., 1950. Characterization of electronic transitions in complex molecules. *Discuss. Faraday Soc.* 9, 14–19.
- Kelly, M.M., Arnold, W.A., 2012. Direct and indirect photolysis of the phytoestrogens genistein and daidzein. *Environ. Sci. Technol.* 46, 5396–5403.
- Li, Y.J., Chen, J.W., Qiao, X.L., Zhang, H.M., Zhang, Y.N., Zhou, C.Z., 2016a. Insights into photolytic mechanism of sulfapyridine induced by triplet-excited dissolved organic matter. *Chemosphere* 147, 305–310.
- Li, Y., Zhang, R., Du, L., Zhang, Q., Wang, W., 2016b. Catalytic mechanism of C-F bond cleavage: insights from QM/MM analysis of fluoroacetate dehalogenase. *Catal. Sci. Technol.* 6, 73.
- Lin, S.H., 1966. Rate of interconversion of electronic and vibrational energy. *J. Chem. Phys.* 44 (10), 3759–3767.
- Louis, F., Gonzalez, C.A., Huie, R.E., 2000. An ab initio study of the kinetics of the reactions of halomethanes with the hydroxyl radical. 1. CH_2Br_2 . *J. Phys. Chem. A* 104 (13), 2931–2938.
- Maudens, K.E., Zhang, G.F., Lambert, W.E., 2004. Quantitative analysis of twelve sulfonamides in honey after acidic hydrolysis by high-performance liquid chromatography with post-column derivatization and fluorescence detection. *J. Chromatogr. A* 1047 (1), 85–92.
- Niu, Y., Peng, Q., Shuai, Z.G., 2008. Promoting-mode free formalism for excited state radiationless decay process with Duschinsky rotation effect. *Sci. China Ser. B* 51 (12), 1153–1158.
- Niu, Y., Peng, Q., Deng, C., Gao, X., Shuai, Z.G., 2010. Theory of excited state decays and optical spectra: application to polyatomic molecules. *J. Phys. Chem. A* 114 (30), 7817–7831.
- Nozaki, K., Takamori, K., Nakatsugawa, Y., Ohno, T., 2006. Theoretical studies of phosphorescence spectra of tris(2,2'-bipyridine) transition metal compounds. *Inorg. Chem.* 45 (16), 6161–6178.
- Peng, Q., Yi, Y., Shuai, Z.G., Shao, J., 2007. Toward quantitative prediction of molecular fluorescence quantum efficiency: role of Duschinsky rotation. *J. Am. Chem. Soc.* 129 (30), 9333–9339.
- Peng, Q., Niu, Y., Shi, Q., 2013. Correlation function formalism for triplet excited state decay: combined spin-orbit and nonadiabatic couplings. *J. Chem. Theory Comput.* 9 (2), 1132–1143.
- Schwaiger, I., Schuch, R., 2000. Bound sulfathiazole residues in honey - need of a hydrolysis step for the analytical determination of total sulfathiazole content in honey. *Dtsch. Lebensm.* 96 (3), 93–98.
- Schwarzenbach, R.P., Escher, B.L., Fenner, K., Hofstetter, T.B., Johnson, C.A., Von Gunten, U., Wehrli, B., 2006. The challenge of micropollutants in aquatic systems. *Science* 313 (5790), 1072–1077.
- Shah, S., Hao, C., 2016. Density functional theory study of direct and indirect photodegradation mechanisms of sulfameter. *Environ. Sci. Pollut. Res.* 23, 19921–19930.
- Shah, S., Zhang, H., Song, X., Hao, C., 2015. Quantum chemical study of the photolysis mechanisms of sulfachloropyridazine and the influence of selected divalent metal ions. *Chemosphere* 138, 765–769.
- Silva-Junior, M.R., Schreiber, M., Sauer, S.P.A., Thiel, W., 2008. Benchmarks for electronically excited states: time-dependent density functional theory and density functional theory based multireference configuration interaction. *J. Chem. Phys.* 129 (10), 104–103.
- Stoev, G., Michailova, A., 2000. Quantitative determination of sulfonamide residues in foods of animal origin by high-performance liquid chromatography with fluorescence detection. *J. Chromatogr. A* 871 (1), 37–42.
- Sun, Y., Zhang, Q., Wang, H., Wang, W., 2015. OH radical-initiated oxidation degradation and atmospheric lifetime of N-ethylperfluorobutyramide in the

- presence of O₂/NO_x. Chemosphere 134, 241–324.
- Te Velde, G., Bickelhaupt, F.M., van Gisbergen, S.J.A., Fonseca Guerra, C., Baerends, E.J., Snijders, J.G., Ziegler, T., 2001. Chemistry with ADF. J. Comput. Chem. 22, 931–967.
- Tomasi, J., Mennucci, B., Cammi, R., 2005. Quantum mechanical continuum solvation models. Chem. Rev. 105 (8), 2999–3093.
- Van Lenthe, E., Van Leeuwen, R., Baerends, E.J., Snijders, J.G., 1993. Relativistic regular two-component Hamiltonians. J. Chem. Phys. 99 (6), 4597–4610.
- Van Lenthe, E., Baerends, E.J., Snijders, J.G., 1994. Relativistic total energy using regular approximations. J. Chem. Phys. 101 (11), 9783–9792.
- Van Lenthe, E., Snijders, J.G., Baerends, E.J., 1996a. The zero-order regular approximation for relativistic effects: the effect of spin-orbit coupling in closed shell molecules. J. Chem. Phys. 105 (15), 6505–6516.
- Van Lenthe, E., van Leeuwen, R., Baerends, E.J., Snijders, J.G., 1996b. Relativistic regular two-component Hamiltonians. Int. J. Quantum Chem. 57 (3), 281–293.
- Van Lenthe, E., Ehlers, A.E., Baerends, E.J., 1999. Geometry optimization in the zero order regular approximation for relativistic effects. J. Chem. Phys. 110 (18), 8943–8953.
- Wang, X.H., Lin, A.Y.C., 2012. Phototransformation of cephalosporin antibiotics in an aqueous environment results in higher toxicity. Environ. Sci. Technol. 46, 12417–12426.
- Wei, X.X., Chen, J.W., Xie, Q., Zhang, S.Y., Ge, L.K., Qiao, X.L., 2013. Distinct photolytic mechanisms and products for different dissociation species of ciprofloxacin. Environ. Sci. Technol. 47 (9), 6746–6755.
- Yan, S., Song, W., 2014. Photo-transformation of pharmaceutically active compounds in the aqueous environment: a review. Environ. Sci. Process. Impacts 16, 697–720.
- Zepp, R.G., Cline, D.M., 1977. Rates of direct photolysis in aquatic environment. Environ. Sci. Technol. 11 (4), 359–366.